Desalination and Water Treatment
www.deswater.com

doi: 10.5004/dwt.2020.24793

174 (2020) 98–105
January

Decomposition of humic acid by ozone: oxidation properties and water-matrix constituents

Peng Wen[a,b], Dan Liu[a], Weiming Chen[a], Guobin Jiang[a], Qibin Li[a,*]

[a]*Faculty of Geosciences and Environmental Engineering, Southwest Jiaotong University, Chengdu 611756, China,*
Tel. +86-13668177795; emails: liqb@home.swjtu.edu.cn (Q.B. Li), 910261687@qq.com (P. Wen), 98749991@qq.com (D. Liu),
chenwm@my.swjtu.edu.cn (W.M. Chen), 645334935@qq.com (G.B. Jiang)
[b]*Enrollment and Allocation Department, Southwest Jiaotong University, Chengdu 611756, China*

Received 2 July 2018; Accepted 16 August 2019

ABSTRACT

Wastewater often contains humic acid (HA) and inorganic anions together. We studied the oxidation properties of high concentration HA in an ozone system and effects of different mass concentrations of CO_3^{2-}, HCO_3^-, SO_4^{2-}, Cl^-, NO_2^- and NO_3^- on the ozonation of HA were investigated. After 30 min, the color number, HA, chemical oxygen demand (COD) and total organic carbon were considerably eliminated, the ozone use decreased significantly and the biodegradability ratio of biochemical oxygen demand (BOD_5)/COD increased from an influent 0.23 to 0.52. Also, the UV-visible spectrum and three-dimensional excitation and emission matrix fluorescence spectrum tests demonstrated that the HA was significantly decomposed into small molecular matters. Also, common inorganic anions had significant influences during the ozonation process. For a 30 min reaction, and water samples with mass concentrations of CO_3^{2-}, HCO_3^-, Cl^- and NO_2^- of 0.5–3.0, 5.0–20.0, 5.0–20.0 and 0.1–0.8 g L^{-1}, respectively, the removal rates of HA were reduced by 8.36%–16.40%, 2.95%–8.85%, 0.66%–3.28% and 10.16%–16.06% respectively, compared with water samples without these anions, and the apparent kinetic constants k_{obs} were 13.88–9.51, 14.59–11.31 and 16.67–14.20 min^{-1}; for water samples with SO_4^{2-} and NO_3^- mass concentrations of 0.5–2.0 and 2.0–8.0 g L^{-1}, the removal rates of HA increased by 2.30%–10.16% and 2.30%–7.54%, and k_{obs} were 17.71–23.85 and 17.9–21.19 min^{-1}. Ozonation could be inhibited by CO_3^{2-}, HCO_3^-, Cl^- and NO_2^-, and the depressions increased as the input increased, however, there is some facilitation when SO_4^{2-} and NO_3^- exist, and the degradation could be accelerated as the input increased.

Keywords: Negative ion/anion; Ozone; Humic acid; Effects; Kinetics

---

1. Introduction

Ozone has mild requirements for reaction and causes no secondary pollution, are known for the ability to mineralize a wide range of organic compounds [1,2]. Duo to the fact that ozone is a powerful oxidant and can decompose organic matter mainly by direct oxidation and hydroxyl radical reaction [3–6]. Also, processes that are combined with ozone have been applied in the rapid pre-oxidation of refractory industrial wastewater. This sort of technology has enabled biological methods to serve as a subsequent treatment [7,8]. Consequently, ozonation technologies have been applied gradually in advanced oxidation processes (AOPs) of reclaimed water from municipal solid-waste plants and industrial plants [3,9–13].

Recently, an excellent ozone oxidization treatment efficiency has been achieved for concentrated leachate with a complicated structure, high-concentrated organics, and a

---

* Corresponding author.

high salinity, in that its biodegradability could be improved [14]. In terms of the impact that high concentrations of anions could have on AOPs, some studies have found that inorganic anions (NO_3^-, HCO_3^-/CO_3^{2-}, and H_2PO_4) in the sonochemical Fe^0-catalyzed persulfate system where sulfadiazine was decomposed influenced the removal efficiency, primarily as a result of the anion ability to react with radicals, which interferes with pollutant removal [15–18]. Also, some studies have found that common anions (HCO_3^-, CO_3^{2-}, Cl^-, NO_3^- and SO_4^{2-}) in water could delay thermal activation [15,17]. Concentrated leachate has often been regarded as a representative of refractory organic wastewater because of its high color number (CN), salinity and organics content, which also has a complex composition and low biodegradability [19,20]. Since high-concentrated anions exist in landfill leachate and anion concentration and type are key parameters that could affect the AOPs. However, to our best knowledge, insufficient research exists on their influence on the course of landfill leachate degradation.

As we all know, humic acid (HA) is main refractory content in landfill leachate and we use it as a simulated leachate organic matter. In the current study, we aimed to (1) investigate the oxidation properties of ozone on HA by analyzing pH, biodegradability and the alkalinity, (2) study the degradation characteristics of HA by ultraviolet-visible (UV-Vis) and three-dimensional excitation and emission matrix fluorescence (3D-EEM), and (3) explore the impacts of CO_3^{2-}, HCO_3^-, SO_4^{2-}, Cl^-, NO_2^- and NO_3^- on ozonation process.

2. Material and methods

2.1. Materials

HA solution (2.00 g L^{-1}) was prepared by dissolving HA in a certain amount of NaOH solution (0.05 mol L^{-1}), filtering it through a 0.45 μm membrane, adjusting the pH to 8.00 ± 0.50 and conditioning by using secondary reverse osmosis water. A simulated HA wastewater sample was studied by 3D-EEM, where the fluorescence peak position is the same as that of leachate, and thus the experimental samples represent HA. HA was from Aladdin Co. (United States), sodium chloride (NaCl), sodium sulfate (Na_2SO_4), sodium nitrate ($NaNO_3$), sodium carbonate (Na_2CO_3), sodium bicarbonate ($NaHCO_3$), sulfuric acid (H_2SO_4) and sodium hydroxide (NaOH) were of analytic grade and were from KeLong Co., Chengdu.

2.2. Experimental method

The oxygen flowrate as provided by a pure oxygen cylinder was controlled by using a rotameter. Ozone, as produced by an ozone generator (3S-T3, Tonglin Technology Co. Ltd., Beijing, China) was continuously sparged into the reactor (1.0 m high, 3 L volume) by a fine bubble diffuser. An ozone concentration analyzer (UV-200T, IDEAL Co. Ltd., USA) was applied to determine the ozone concentration and an ozone destruction apparatus, which was used to match products with the ozone concentration analyzer, was applied to eliminate ozone and to prevent secondary air pollution.

Synthetic HA wastewater (2.0 L) was injected into a 3.0 L reactor and the HA concentration was determined before and after addition at a set time. Based on the detected concentration of anions in the landfill leachates (Table 1), the mass concentrations of CO_3^{2-}, HCO_3^-, SO_4^{2-}, Cl^-, NO_2^-, and NO_3^- were controlled to a set value and the initial sample pH was adjusted. During the reaction for 2, 5, 10, 15, 20, 25 and 30 min, samples were adjusted to pH 8.0 and heated for 30 min in a 50°C water bath to eliminate interference from residual ozone. In this study, k_{obs} were to present the reaction rate and were fitted by the pseudo-first-order kinetic model.

2.3. Analytical method

Chemical oxygen demand (COD) was determined by the dichromate method (GB 11914-89). 5 d biochemical oxygen demand (BOD_5) was determined by the speedy testing method of the microorganism sensor (HJ/T 86-2002). A multifunctional 2100 total organic carbon (TOC)/total nitrogen analyzer (Germany Analytik Jena AG Corporation, Germany) was used to determine TOC. Oxidation-reduction potential (ORP) was detected by the ORP transmitter (JENCO 6TX) with an ORP electrode (JENCO 6TX, United States). The CN as defined by Eq. (1) was to characterize color. A_{436}, A_{525}, and A_{620} present the absorbance at a wavelength of 436, 525 and 620 nm, respectively [21].

$$\mathrm{CN} = \frac{A_{436}^2 + A_{525}^2 + A_{620}^2}{A_{436} + A_{525} + A_{620}} \tag{1}$$

Table 1
Landfill leachates characteristics and anion concentrations

Samples[a]	Leachate characteristics			Anion species and concentrations					
	pH	COD	NH_3–N	Cl^-	SO_4^{2-}	HCO_3^-	CO_3^{2-}	NO_3^-	NO_2^-
1#	7.92	2,854.9	43.6	13,883.7	2,43.7	3,716.9	923.2	8,842.1	110.2
2#	8.67	6,736.8	83.1	16,458.6	760.7	19,080.8	1,876.8	2,641.8	821.8
3#	7.67	2,854.9	20.1	16,458.6	1,055.2	3,099.5	750.9	7,637.7	354.6
4#	7.96	1,000.0	34.2	5,100.7	420.5	18,002.2	2,953.2	29.4	2.5
5#	7.56	2,659.3	1,836.0	8,200.6	580.8	19,259.2	3,452.5	52.4	120.5
Test value	8.5–11	1,400	200–800	5,000–20,000	500–2,000	5,000–20,000	500–3,000	2,000–8,000	100–800

[a] Besides pH, the units are mg L^{-1}; 1#, 2#, 3# represent concentrated leachate from three landfills, 4# represents leachate from a semi-aerobic laboratory bioreactor, 5# represents leachate from a regulating tank in a landfill.

Ozone dosage was controlled to be 65 mg L^{-1} by a flowmeter and digitally displayed by an ozone analyzer (IDEAL UV-200T, U.S.A.). At the end of the experiment setup, an ozone destroyer (IDEAL matching device) was applied to consume outflow ozone. The ozone utilization rate of the process was defined by Eq. (2). Where 65 and C_t are ozone concentration (mg L^{-1}) at a reaction time of 0 min and during specific reaction time (t). It was measured in the gas phase (from the ozone monitors) and R presents the ozone utilization rate.

$$R = \frac{\left(65 - C_t\right)}{65} \tag{2}$$

Anion mass concentrations were detected using ion chromatography (ICS-1100, DIONEX Co. Ltd., USA) with an anion-exchange chromatographic column (IonPac AS23, DIONEX Co. Ltd., USA). The three-dimensional fluorescence spectrum of HA was detected using a synchronous absorption three-dimensional fluorescence spectrometer. The HA concentration was represented by absorbance at 254 nm, which will be abbreviated as UV_{254}. The UV-Vis spectra were measured directly by spectrophotometer (Lambda 950, Perkin-Elmer Co. Ltd, USA). The concentration of HA can be determined according to the concentration from an HA-absorbance standard curve (Eq. 3). A glass-electrode method was applied to determine the pH and the pH of samples was detected by a pH meter.

$$Y = 3.5359X + 0.0176 \ \left(R^2 = 0.9999\right) \tag{3}$$

where X is the concentration of HA (mg L^{-1}) and Y is the absorbance value.

3. Results and discussion

3.1. Characteristics of ozone-oxidizing HA

3.1.1. Removal efficiencies of organics

Fig. 1a shows that the removal efficiencies of CN, HA, the COD and TOC increased with time and displayed a linear behavior with reaction time. At 30 min, the removal efficiencies of CN, HA, COD and TOC were considerable eliminated (model fitting formula: $y = e^{-0.5704x}$, $y = e^{-0.0772x}$, $y = e^{-0.0541x}$ and $y = e^{-0.0309x}$), respectively. The three indices followed the numerical relation, CN removal efficiency > HA > COD > TOC, and was nearly proportional, which indicates that the chromogenic group of humic-like substances was destroyed, the unsaturated chromophore bond exhibited a 1,3-dipolar cycloaddition and the reaction was severe, and the hydroxyl radicals oxidized macromolecular organic matter to small molecular organic matter or even mineralized it [7,10]. By-products accumulated gradually with reaction time, such as carboxylic acid intermediates, which exist in the molecular form under acidic conditions and hydrogen bonds, which exist intra- and intermolecularly, and thus, the reaction resistance increased and the reaction rate decreased. As the reaction continued, the amount of HAs and the pH decreased and the number of carboxylic acid intermediates increased, which lead to an increase of effluent residual ozone concentration and a decrease in its contribution to a decreased HA removal (Fig. 1d). The system ORP increased with a smaller range in the first 20 min of the reaction, whereas the increase was relatively significant in the later reaction stage (Fig. 1c).

As shown in Fig. 1b, the biodegradation of simulated wastewater improved gradually with reaction time and the value of BOD_5/COD increased gradually with time. After oxidizing with ozone for 30 min, the BOD_5/COD of the simulated wastewater improved from 0.23 (inlet) to 0.52. The ozone and hydroxyl radicals can degrade macromolecular refractory organic matter to intermediates, which may favor microorganism degradation and utilization. As the reaction time proceeded, the concentration of bicarbonate in the HA solution kept increasing and the pH showed a downward trend. During the first 5 min of reaction time, the bicarbonate concentration showed a linear increase, and 30 min into the reaction, the bicarbonate concentration increased from 32.67 to 405.72 mg L^{-1} because the ozone and hydroxyl radicals that were generated by ozone have a strong oxidation effect on macromolecular refractory organic matter in the system. Some small molecular organic acids were generated after the degradation of HA and the pH of simulated wastewater lead to a continuous decrease.

3.1.2. Aromaticity and humification degree analysis

UV-Vis was widely applied in many types of research to investigate the aromaticity and humification degree [10,20,22,23]. As shown in Fig. 2, UV_{254} and E_{280} decreased with an increase in reaction time. After being treated with ozone for 30 min, UV_{254} decreased gradually from 0.59 (inlet) to 0.05 and E_{280} decreased gradually from 0.51 (inlet) to 0.04, which shows that ozonation can decrease the aromaticity of HA significantly. E_{300}/E_{400} increased gradually with reaction time. After being treated by ozone for 30 min, E_{300}/E_{400} increased gradually from 2.56 (inlet) to 4.44, which shows that the humification of simulated wastewater treated by ozone decreased gradually. The humification of HA is linear with the degree of aromaticity, which is consistent with the study by He et al. [20]. From the above, we can see that the humification degree of HA is linear with an aromaticity degree, which is consistent with previous studies [3,8]. It is also noteworthy that HA had an obvious acromion at a wavelength of 260 nm, acromion got weakened with the increase of reaction time, which showed that degradable components were increasing and the structure of HA tended to be simple.

3.1.3. HA degradation analysis

3D-EEM also was popular to determine the fluorescence degree and molecular weight of organics [22,24]. Fig. 3 shows that the 3D-EEM spectrum of HA-simulated wastewater had three main luminous regions, including Flu1 (Ex/Em = 310–360 nm/370–450 nm), which is fluorescence of humic-like acid in the visible region; Flu2 (Ex/Em = 220–230 nm/300–350 nm), which is fluorescence of tryptophan-like components at low excitation wavelengths; Flu3 (Ex/Em = 235–255 nm/410–500 nm), which is fluorescence of humic-like acid in the ultraviolet region [20,25]

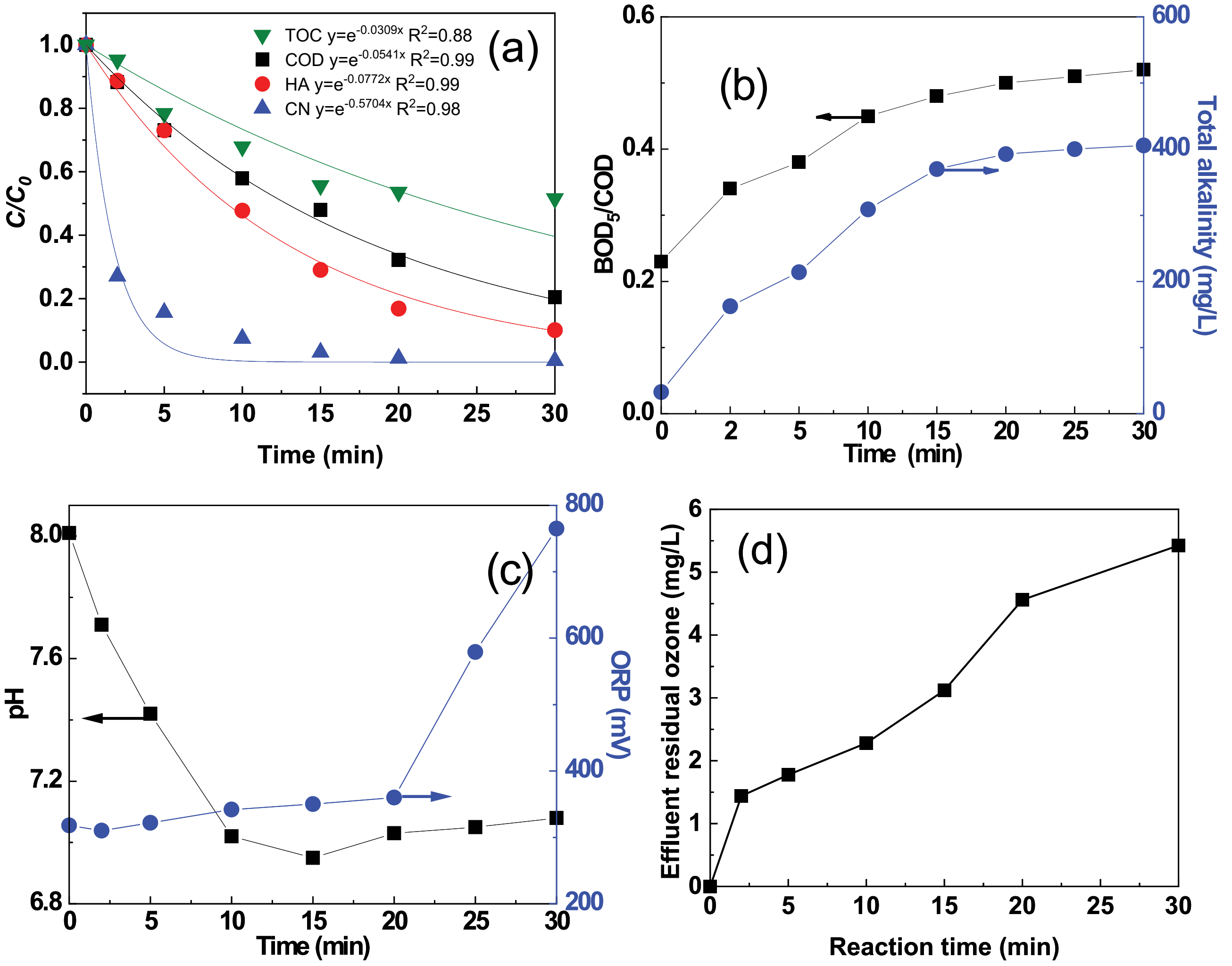

Fig. 1. Effluents properties over time: (a) TOC, COD, UV_{254} and CN C/C_0 of organics, (b) variation of BOD_5/COD value and total alkalinity over time, (c) variation of pH and ORP over time and (d) effluent residual ozone concentration. Conditions: $[O_3]$ constant = 65.0 ± 0.5 mg L^{-1}, $[HA]_0$ = 2 g L^{-1}, initial pH = 7.80 ± 0.10.

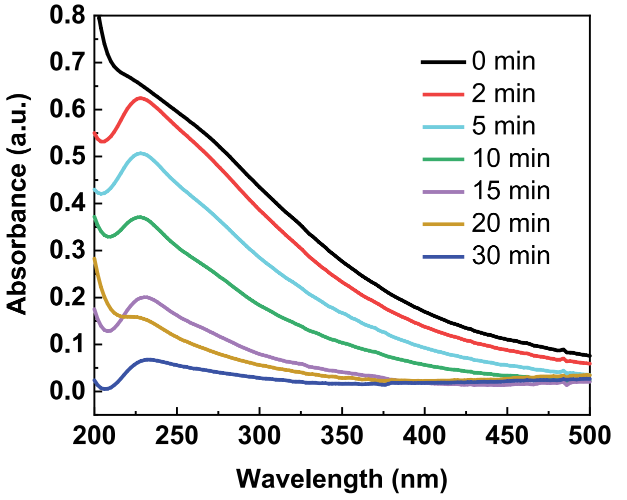

Fig. 2. UV-Vis spectra of HA in the ozone process in different reaction times.

Baker et al. [23] pointed out that fluorescence of humic-like acid in the ultraviolet region was caused mainly by organic matter with low molecular weight but a high fluorescence efficiency; fluorescence of humic-like acid in the visible region was produced by aromatic substances with a relatively stable and high molecular weight. The simulated wastewater produced a greater fluorescence intensity in Flu3, which shows that this simulated wastewater can represent humic-like acid refractory wastewater. When the reaction time was 30 min, the peak value in Flu3 decreased obviously. The peak position of Ex/Em blue-shifted from 270 nm/460 nm to 260 nm/450 nm, which shows that refractory humic-like acid in the ultraviolet region is oxidized rapidly by ozone; the molecular structure of HA could be destroyed quickly and the molecular condensation degree, aromatic degree, and humification degree decreased. Furthermore, although the tryptophan-like components were accumulated during the reaction (e.g. 5 min), the intensity of the Flu2 also tends to decrease in the late stage which might be attributed to the mineralization ability of hydroxyl radicals.

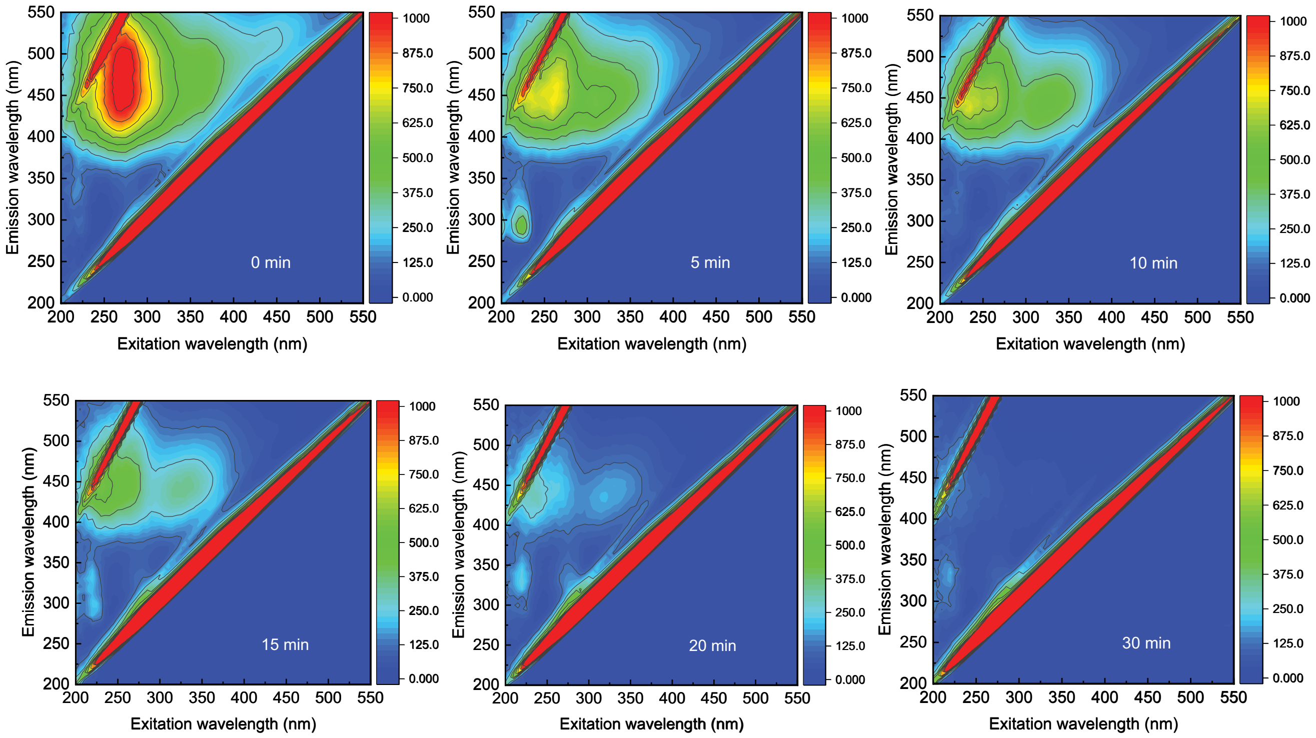

Fig. 3. 3D-EEM spectrum of HA in the ozonation process in different reaction times.

After a comprehensive analysis of the fluorescence indices of HA before and after ozonation, we can see that the π electrons of the system in HA-simulated wastewater changed systematically after ozonation and that the aromatic nucleus of the HA decreased and oxidized to small molecular matter. The 3D-EEM spectrum indicates that ozone can degrade macromolecule humic-like acid matters and mineralize small-molecular-weight tryptophan, which is consistent with UV-Vis analysis and conclusions conducted by BOD$_5$.

3.2. Interruption of inorganic anions

3.2.1. Effects of CO_3^{2-} and HCO_3^- on ozonation

On the precondition that no mutual transformation occurs between CO_3^{2-} and HCO_3^- in the initial state, with the distribution fraction of CO_3^{2-} under different conditions of pH taken into consideration, the pH for the initial system of CO_3^{2-} and HCO_3^- was set at 11.00 and 8.50, respectively, and the correlative coefficient of the fitted equation of the reaction rate exceeded 98.08% with no exception, as shown in Fig. 4.

As shown in Fig. 4, when the initial concentration of CO_3^{2-} increased from 0 to 3.0 g L^{-1}, the removal rate of HA decreased by 8.36%–16.40% and k_{obs} were reduced from 13.88 to 9.51 min^{-1}. When the initial concentration of HCO_3^- increased from 0 to 20.0 g L^{-1}, the removal rate of HA decreased by 2.95%–8.85%, and k_{obs} were reduced from 14.59 to 11.31 min^{-1}. Therefore, CO_3^{2-} and HCO_3^- have a strong inhibitory effect on ozonation.

The removal rate of HA at the same reaction time dropped as the concentration of CO_3^{2-} and HCO_3^- increased. CO_3^{2-} and HCO_3^- could react with hydroxyl radicals with electron transfer (Eqs. (4) and (5)) [26]. The reduced concentration of hydroxyl radicals that are caused by an electron-transfer reaction could lower the contact probability between the hydroxyl radical and HA, and the removal rate of HA decreased gradually. $CO_3^{\bullet-}$ and $HCO_3^{\bullet-}$ that were generated in the system were less easily oxidized compared with $OH^{\bullet-}$, which could lower the system ORP, and prevent HA removal. This result matches that where CO_3^{2-} and HCO_3^- can remove $SO_4^{\bullet-}$ rapidly in the Fe^0-catalyzed persulfate system where sulfadiazine was decomposed [27].

$$^{\bullet}OH + HCO_3^- \rightarrow OH^- + {}^{\bullet}HCO_3 \qquad K = 1.5 \times 10^7\,M^{-1}s^{-1} \tag{4}$$

$$^{\bullet}OH + CO_3^{2-} \rightarrow OH^- + {}^{\bullet}CO_3^- \qquad K = 4.2 \times 10^8\,M^{-1}s^{-1} \tag{5}$$

3.2.2. Effects of SO_4^{2-} and Cl^- on ozonation

High concentrations of sulfate and chloride ions exist in landfill leachate and their effect on ozonation was studied by adding various quantities of sodium sulfate and sodium chloride into the HA matrix, with an initial pH of 9.5. The results are shown in Fig. 5.

According to Fig. 5, when the initial concentration of SO_4^{2-} increased from 0 to 2.0 g L^{-1}, the HA removal rate increased from 38.36% to 48.52% after 30 min, and k_{obs} increased from 17.71 to 23.85 min^{-1}. The HA removal rate at the same reaction time increased as the concentration of SO_4^{2-} increased because an electron-transfer reaction occurred between the hydroxyl and sulfate radicals (Eqs. (6)–(8)) [28,29]. The sulfate radical with a relatively high

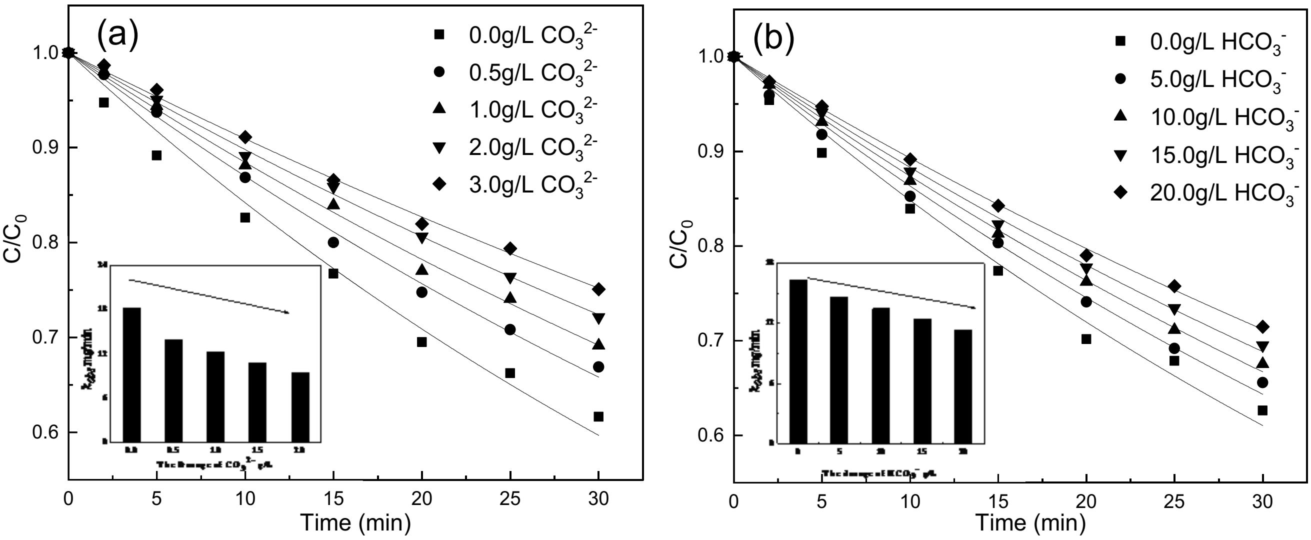

Fig. 4. Effects on the oxidation kinetics of HA in the ozone system by CO_3^{2-} and HCO_3^- at various concentrations.

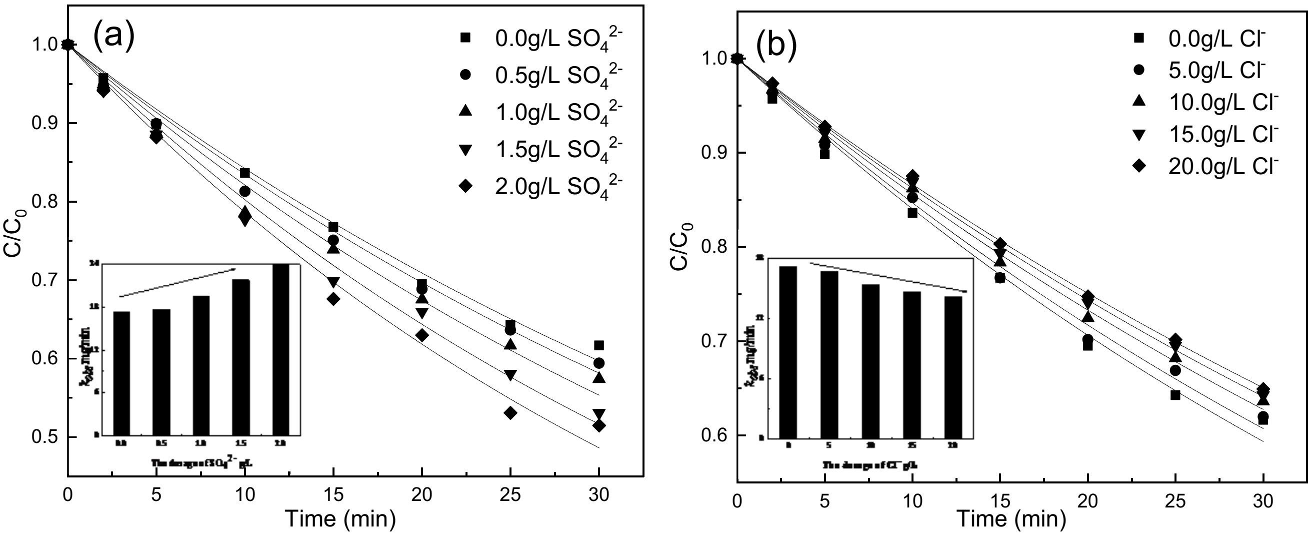

Fig. 5. Effects on the oxidation kinetics of HA in the ozone system with SO_4^{2-} and Cl^- at various concentrations.

ORP (E_0 = 2.5–3.1 V), was assumed to be able to oxidize most organic matter under ideal conditions. Compared with the hydroxyl radical, the sulfate radical could last longer once produced, thus its existence could improve the system ORP and the contact probability between the oxidants and the organics, and enhance the HA removal efficiency. The ability for oxidation in the SO_4^{2-} ozone system was strengthened through complex oxidization by sulfate and hydroxyl radicals, and the ability of the ozonation system to decompose HA was improved by SO_4^{2-}.

$$SO_4^{2-} + {}^{\bullet}OH \rightarrow SO_4^{\bullet-} + OH^- \tag{6}$$

$$SO_4^{2-} + SO_4^{\bullet-} \rightarrow S_2O_8^{2-} + e^- \tag{7}$$

$$S_2O_8^{2-} \rightarrow 2SO_4^{\bullet-} \tag{8}$$

$$SO_4^{\bullet-} + HS \rightarrow \text{organic intermediates} \tag{9}$$

$$SO_4^{\bullet-} + \text{organic intermediates} \xrightarrow{\text{fast}} CO_2 + H_2O \tag{10}$$

According to Fig. 5, when the initial concentration of Cl^- increased from 0 to 20.0 g L^{-1}, the HA removal rate dropped from 38.36 % to 35.08 % after 30 min, and k_{obs} decreased from 14.59 to 11.31 min^{-1}, which is lower than that for cases where other ions were studied. As the reaction continued, the HA removal rate decreased with an increasing concentration of Cl^-. Hydroxyl radicals and ozone can react with Cl^-, however, a rapid reaction occurred between Cl^- and the hydroxyl radical, and produced unstable reaction products, so it is speculated that Cl^- consumed hydroxyl radicals constantly and may cause a circulation of consumption (Eqs. (11)–(13)) [21]. Reactions between ozone and Cl^- were processed slowly. The ORP of generated $Cl_2^{\bullet -}$ ($E_{(Cl_2^{\bullet -}/Cl^-)} = 2.0$ V) and $Cl^\bullet$ ($E_{(Cl^\bullet/Cl^-)} = 2.4$ V) was lower than that of $^\bullet OH$ (2.8 V) (Eqs. (14)–(17)) [18,30]. Therefore, a cycled consumption with hydroxyl radicals and processes produced matter with a lower ORP, and the Cl^- could reduce the HA removal rate slightly and yield a small decrease. In the system with concentrated Cl^-, intermediate products may change into contaminants with chlorinated organics, which could increase the wastewater biotoxicity.

$$^\bullet OH + Cl^- \leftrightarrow ClOH^{\bullet -} \qquad k_f = 6.1 \pm 0.8 \times 10^9\,L\,mol^{-1}s^{-1} \tag{11}$$

$$O_3 + Cl^- \rightarrow O_2 + OCl^- \qquad k = 0.003\,L\,mol^{-1}\,s^{-1} \tag{12}$$

$$O_3 + OCl^- \rightarrow 2O_2 + Cl^- \qquad k = 110\,L\,mol^{-1}\,s^{-1} \tag{13}$$

$$Cl^- + Cl^\bullet \leftrightarrow Cl_2^{\bullet -} \qquad k_f = 8.0 \times 10^9\,M^{-1}\,s^{-1} \tag{14}$$

$$Cl_2^{\bullet -} + H_2O \rightarrow ClOH^{\bullet -} + {}^\bullet Cl^- + H^+ \qquad k = 1.3 \times 10^3 s^{-1} \tag{15}$$

$$Cl_2^{\bullet -} + Cl_2^{\bullet -} \rightarrow Cl_2 + 2Cl^- \qquad k = 1.3 \times 10^9 M^{-1}s^{-1} \tag{16}$$

$$^\bullet OH + Cl_2^{\bullet -} \rightarrow HOCl + Cl^- \qquad k = 1.0 \times 10^9 M^{-1}s^{-1} \tag{17}$$

3.2.3. Effect of NO_2^- and NO_3^- on ozonation

Various quantities of sodium nitrites and sodium nitrates were added for nitrite oxidation by ozone and hydroxyl radicals in pH 9.5 wastewater, to investigate the influence and competition mechanisms of HA ozonation by nitrite and nitrate ions. The results are shown in Fig. 6.

According to Fig. 6, when the initial concentration of NO_2^- increased from 0 to 0.8 g L^{-1}, the HA removal rate decreased from 38.36% to 22.30% after 30 min and decreased by as much as 16.06%. k_{obs} decreased from 16.67 to 14.20 min^{-1}, which is lower than that where other ions were studied. This occurred because the nitrites could react rapidly with hydroxyl radicals and produce nitrates with hydroxyl radicals and ozone (Eqs. (18)–(20)) [21]. HA competed with nitrites for hydroxyl radicals and ozone, which lead to a decrease in the HA removal rate with an increase in nitrate concentration.

According to Fig. 6, when the initial concentration of NO_3^- increased from 0 to 2.0 g L^{-1}, the HA removal rate increased from 38.36 % to 42.30% after 30 min, and k_{obs} increased slightly from 17.90 to 21.19 min^{-1}. Nitrate with hydroxyl radicals can generate nitrate radicals (Eq. (21)) with an ORP of 2.0–2.2 V [21]. In this study, so that HA could be oxidized by hydroxyl radical and nitrate radicals, improving the removal rate of HA as the concentration of nitrite increased as well. We proposed that $NO_3^\bullet$ had a relative long existence time than hydroxyl radical, increasing reaction time with HA, a consequence that HA degradation rate enhanced slightly as NO_3^- concentration increasing. Therefore, HA can be oxidized by hydroxyl and nitrate radicals and improve the HA removal rate as the nitrite concentration increased. Hereinto, the mechanism should be further studied.

$$NO_2^- + {}^\bullet OH \rightarrow NO_2^\bullet + OH^- \qquad k = 1 \pm 0.1 \times 10^{10} M^{-1}s^{-1} \tag{18}$$

$$2NO_2^\bullet \rightarrow N_2O_4 \qquad k = 9 \times 10^8 M^{-1}s^{-1} \tag{19}$$

$$N_2O_4 + H_2O \rightarrow NO_2^- + NO_3^- \qquad k = 9.5 \times 10^9 M^{-1}s^{-1} \tag{20}$$

$$NO_3^- + {}^\bullet OH \rightarrow NO_3^\bullet + OH^- \qquad k < 5 \times 10^5 M^{-1}s^{-1} \tag{21}$$

4. Conclusions

Decomposition mechanisms of a concentrated HA matrix by ozone is a hydroxyl radical-and-ozone-combined oxidation process, with degradation products that consist

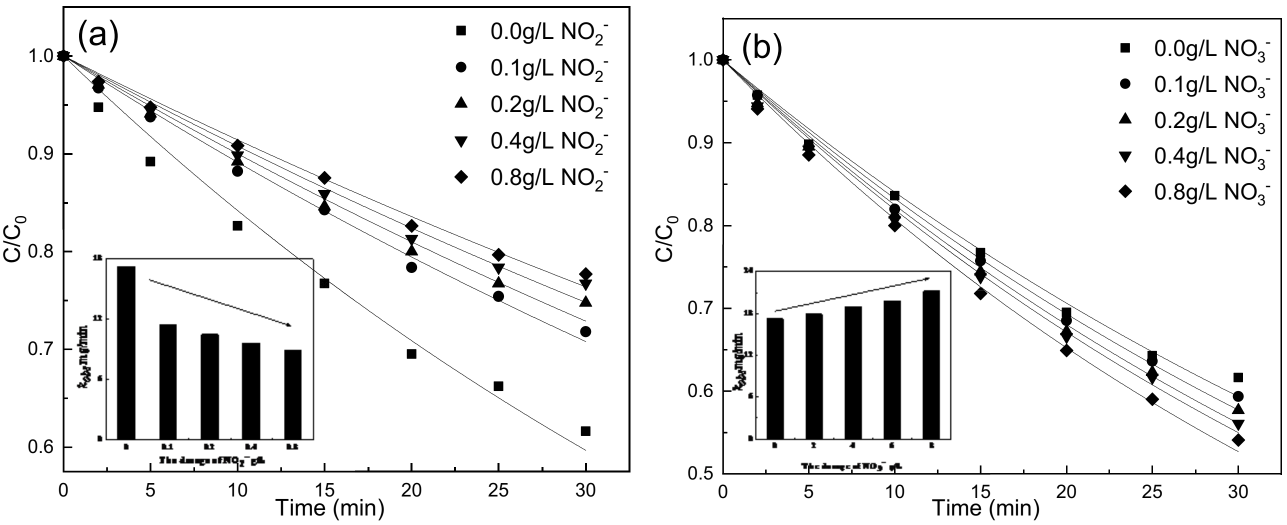

Fig. 6. Effects on the oxidation kinetics of HA in the ozone system by NO_2^- and NO_3^- at various concentrations.

mainly of small molecular alkane. Because landfill leachate contains various high concentrations of inorganic anions, the radical reactions between hydroxyl radicals and ozone could lead to fluctuations in the HA removal rate. Carbonate, bicarbonate, chloride ions, ammonia, and nitrite could decrease the HA degradation, and lead to a decrease in HA removal rate compared with the control, with decreases of 8.68%, 8.86%, 3.28%, 15.21% and 16.06%, respectively. The presence of SO_4^{2-} and NO_3^- encourages the formation of a new radical with a stronger oxidation potential, which improves the HA removal rate by 10.16% and 3.94%, respectively, compared with the control.

Acknowledgments

The authors gratefully acknowledge the Foundation of Key Laboratory of Special Waste Water Treatment, Sichuan Province Higher Education System (No. SWWT2015-4).

References

[1] U. von Gunten, Ozonation of drinking water: Part I. Oxidation kinetics and product formation, Water Res., 37 (2003) 1443–1467.

[2] T. Ozge, I. Hatice, D. Anatoli, Experimental study of humic acid degradation and theoretical modelling of catalytic ozonation, Environ. Sci. Pollut. Res. Int., 22 (2015) 202.

[3] S.S.A. Amr, H.A. Aziz, M.N. Adlan, Optimization of stabilized leachate treatment using ozone/persulfate in the advanced oxidation process, Waste Manage., 33 (2013) 1434–1441.

[4] R.J. Qu, B.Z. Xu, L.J. Meng, L.S. Wang, Z.Y. Wang, Ozonation of indigo enhanced by carboxylated carbon nanotubes: performance optimization, degradation products, reaction mechanism and toxicity evaluation, Water Res., 68 (2015) 316–327.

[5] W.R. Haag, J. Hoigné, Ozonation of water containing chlorine or chloramines. Reaction products and kinetics, Water Res., 17 (1983) 1397–1402.

[6] S.Y. Wang, X.H. Wang, J. Chen, R.J. Qu, Z.Y. Wang, Removal of the UV filter benzophenone-2 in aqueous solution by ozonation: kinetics, intermediates, pathways and toxicity, Ozone Sci. Eng., 40 (2017) 122–132.

[7] F. Daoud, D. Pelzer, S. Zuehlke, M. Spiteller, O. Kayser, Ozone pretreatment of process waste water generated in course of fluoroquinolone production, Chemosphere, 185 (2017) 953–963.

[8] N. Amaral-Silva, R.C. Martins, S. Castro-Silva, R.M. Quinta-Ferreira, Ozonation and perozonation on the biodegradability improvement of a landfill leachate, J. Environ. Chem. Eng., 4 (2016) 527–533.

[9] N.M. Ghazi, A.A. Lastra, M.J. Watts, Hydroxyl radical ($^\bullet$OH) scavenging in young and mature landfill leachates, Water Res., 56 (2014) 148–155.

[10] H.-W. Wang, X.-Y. Li, Z.-P. Hao, Y.-J. Sun, Y.-N. Wang, W.-H. Li, Y.F. Tsang, Transformation of dissolved organic matter in concentrated leachate from nanofiltration during ozone-based oxidation processes (O_3, O_3/H_2O_2 and O_3/UV), J. Environ. Manage., 191 (2017) 244–251.

[11] S.S.A. Amr, S.N.F. Zakaria, H.A. Aziz, Performance of combined ozone and zirconium tetrachloride in stabilized landfill leachate treatment, J. Mater. Cycles Waste Manage., 19 (2016) 1384–1390.

[12] W.M. Chen, Z.P. Gu, P. Wen, Q.B. Li, Degradation of refractory organic contaminants in membrane concentrates from landfill leachate by a combined coagulation-ozonation process, Chemosphere, 217 (2019) 411–422.

[13] W.M. Chen, A.P. Zhang, Z.P. Gu, Q.B. Li, Enhanced degradation of refractory organics in concentrated landfill leachate by Fe^0/H_2O_2 coupled with microwave irradiation, Chem. Eng. J., 354 (2018) 680–691.

[14] S.S.A. Amr, H.A. Aziz, S. Hossain, M.J.K. Bashir, Simultaneous removal of COD and color from municipal landfill leachate using ozone/zinc Sulphate oxidation process, Global Nest J., 19 (2017) 498–504.

[15] C. Qi, X. Liu, J. Ma, C. Lin, X. Li, H. Zhang, Activation of peroxymonosulfate by base: implications for the degradation of organic pollutants, Chemosphere, 151 (2016) 280–288.

[16] C.D. Qi, X.T. Liu, C.Y. Lin, X.H. Zhang, J. Ma, H.B. Tan, W. Ye, Degradation of sulfamethoxazole by microwave-activated persulfate: kinetics, mechanism and acute toxicity, Chem. Eng. J., 249 (2014) 6–14.

[17] C.D. Qi, X.T. Liu, Y. Li, C.Y. Lin, J. Ma, X.W. Li, H.J. Zhang, Enhanced degradation of organic contaminants in water by peroxydisulfate coupled with bisulfite, J. Hazard. Mater., 328 (2017) 98–107.

[18] G.-D. Fang, D.D. Dionysiou, Y. Wang, S.R. Al-Abed, D.-M. Zhou, Sulfate radical-based degradation of polychlorinated biphenyls: effects of chloride ion and reaction kinetics, J. Hazard. Mater., 227–228 (2012) 394–401.

[19] Y.Y. Long, J. Xu, D.S. Shen, Y. Du, H.J. Feng, Effective removal of contaminants in landfill leachate membrane concentrates by coagulation, Chemosphere, 167 (2017) 512–519.

[20] R. He, X.-M. Wei, B.-H. Tian, Y. Su, Y.-L. Lu, Characterization of a joint recirculation of concentrated leachate and leachate to landfills with a microaerobic bioreactor for leachate treatment, Waste Manage., 46 (2015) 380–388.

[21] C. Tizaoui, L. Bouselmi, L. Mansouri, A. Ghrabi, Landfill leachate treatment with ozone and ozone/hydrogen peroxide systems, J. Hazard. Mater., 140 (2007) 316–324.

[22] Q.Q. Ji, J. Li, Z.K. Xiong, B. Lai, Enhanced reactivity of microscale Fe/Cu bimetallic particles (mFe/Cu) with persulfate (PS) for *p*-nitrophenol (PNP) removal in aqueous solution, Chemosphere, 172 (2016) 10.

[23] A. Baker, M. Curry, Fluorescence of leachates from three contrasting landfills, Water Res., 38 (2004) 2605–2613.

[24] B. Lai, Z.Y. Chen, S.P. Fang, Y.X. Zhou, A combined treatment approach using Fe^0/air and Fenton's reagent for the treatment of delay explosive wastewater, Ind. Eng. Chem. Res., 54 (2015) 7094–7101.

[25] X.S. He, B.D. Xi, Z.M. Wei, X.J. Guo, M.X. Li, D. An, H.L. Liu, Spectroscopic characterization of water extractable organic matter during composting of municipal solid waste, Chemosphere, 82 (2011) 541–548.

[26] C.J. Liang, Z.-S. Wang, N. Mohanty, Influences of carbonate and chloride ions on persulfate oxidation of trichloroethylene at 20°C, Sci. Total Environ., 370 (2006) 271–277.

[27] Z. Tao, X. Zou, J. Mao, X. Wu, Decomposition of sulfadiazine in a sonochemical Fe^0-catalyzed persulfate system: parameters optimizing and interferences of wastewater matrix, Appl. Catal., B, 185 (2016) 31–41.

[28] X.P. Wang, F. Zhang, H.-T. Kung, A. Ghulam, A.L. Trumbo, J.Y. Yang, Y. Ren, Y.Q. Jing, Evaluation and estimation of surface water quality in an arid region based on EEM-PARAFAC and 3D fluorescence spectral index: a case study of the Ebinur Lake Watershed, China, CATENA, 155 (2017) 62–74.

[29] J.L. Wang, S.Z. Wang, Activation of persulfate (PS) and peroxymonosulfate (PMS) and application for the degradation of emerging contaminants, Chem. Eng. J., 334 (2018) 1502–1517.

[30] D.O. Mártire, J.A. Rosso, S. Bertolotti, G.C.L. Roux, A.M. Braun, M.C. Gonzalez, Kinetic study of the reactions of chlorine atoms and $Cl_2^{\bullet-}$ radical anions in aqueous solutions. II. Toluene, benzoic acid, and chlorobenzene, J. Phys. Chem. A, 105 (2001) 5385–5392.